Follow us @BoneJointRes

Freely available online OPEN ACCESS

BJR

CARTILAGE

Regeneration of injured articular cartilage using the recombinant human amelogenin protein

O. Helwa-Shalom,
F. Saba,
E. Spitzer,
S. Hanhan,
K. Goren,
S. I. Markowitz,
D. Shilo,
N. Khaimov,
Y. N. Gellman,
D. Deutsch,
A. Blumenfeld,
H. Nevo,
A. Haze

From Hadassah University Medical Center, Jerusalem, Israel

Aims

Cartilage injuries rarely heal spontaneously and often require surgical intervention, leading to the formation of biomechanically inferior fibrous tissue. This study aimed to evaluate the possible effect of amelogenin on the healing process of a large osteochondral injury (OCI) in a rat model.

Methods

A reproducible large OCI was created in the right leg femoral trochlea of 93 rats. The OCIs were treated with 0.1, 0.5, 1.0, 2.5, or 5.0 µg/µl recombinant human amelogenin protein (rHAM⁺) dissolved in propylene glycol alginate (PGA) carrier, or with PGA carrier alone. The degree of healing was evaluated 12 weeks after treatment by morphometric analysis and histological evaluation. Cell recruitment to the site of injury as well as the origin of the migrating cells were assessed four days after treatment with 0.5 µg/µl rHAM⁺ using immunohistochemistry and immunofluorescence.

Results

A total of 12 weeks after treatment, 0.5 µg/µl rHAM⁺ brought about significant repair of the subchondral bone and cartilage. Increased expression of proteoglycan and type II collagen and decreased expression of type I collagen were revealed at the surface of the defect, and an elevated level of type X collagen at the newly developed tide mark region. Conversely, the control group showed osteoarthritic alterations. Recruitment of cells expressing the mesenchymal stem cell (MSC) markers CD105 and STRO-1, from adjacent bone marrow toward the OCI, was noted four days after treatment.

Conclusion

We found that 0.5 µg/µl rHAM⁺ induced in vivo healing of injured articular cartilage and subchondral bone in a rat model, preventing the destructive post-traumatic osteoarthritic changes seen in control OCIs, through paracrine recruitment of cells a few days after treatment.

Cite this article: *Bone Joint Res* 2023;12(10):615–623.

Keywords: Amelogenin, Articular cartilage, Osteochondral injury

Article focus

- The healing effect of amelogenin on articular cartilage injuries in a rat model.

Key messages

- Amelogenin induced healing of injured articular cartilage and subchondral bone in a rat model of osteochondral injury (OCI).
- Paracrine recruitment of cells into the OCI is an early event correlated with the healing process.

Strengths and limitations

- An accurate and reproducible rat knee OCI model was developed.
- Partial healing of the articular cartilage was demonstrated 12 weeks after treatment with recombinant human

Correspondence should be sent to Amir Haze; email: amir.haze@mail.huji.ac.il

doi: 10.1302/2046-3758.1210.BJR-2023-0019.R1

Bone Joint Res 2023;12(10):615–623.

amelogenin protein. Evaluation of additional time points would be beneficial.
- The molecular mechanisms underlying the induced healing were not deciphered yet.

Introduction

The spontaneous healing capacity of articular cartilage is extremely limited due to its avascular configuration and low metabolic activity.[1] Articular cartilage lesions are painful and may limit strenuous physical activities and, eventually, normal everyday activities.[2] Several cartilage repair techniques have been developed. In stable, non-displaced lesions, nonoperative management is usually the initial treatment modality. However, these treatments have limited success rates and frequently merely delay surgical intervention. The surgical armamentarium – either cell-based strategies, whole-tissue transplantation, or total joint replacement – depends on the size, depth, and location of the lesion.[3] In recent years, the use of mesenchymal stem cells (MSCs) to treat cartilage defects has been widely investigated. MSCs isolated from various mesenchymal tissues were differentiated into chondrocytes and introduced into damaged cartilage in combination with chondrogenic factors and scaffolds. However, exogenous transplantation is restricted by limited MSC sources, excessive manufacturing costs, and technical difficulties. Autologous transplantation is additionaly restricted by the need for two surgical interventions.[3-5]

Previously, we described the expression of amelogenin in bone marrow stromal cells and growth plate chondrocytes.[6] We have also demonstrated that a single application of recombinant human amelogenin protein (rHAM+), produced in our laboratory,[7] induced progressive and significant regeneration of all periodontal tissues after induction of experimental periodontitis in a dog model. No regeneration was detected in the control group treated with the carrier propylene glycol alginate (PGA).[8] Next, we demonstrated that rHAM+ induced regeneration of torn rat skeletal ligaments in a dose-dependent manner: the medial collateral ligament (MCL) (as a proof of concept),[9] and the calcaneofibular ligament (CFL) of the ankle joint (as an unmet clinical need).[10] Transected MCLs and CFLs treated with rHAM+ regained their mechanical strength and structural composition compared to normal ligaments from the contralateral leg, and were significantly stronger than the control groups.[9,10] The single application of rHAM+ increased the number of cells expressing the MSC markers CD105 and STRO-1 in the granulation tissue of periodontal defect, and transected MCL models several days after treatment.[8,9]

Based on our previous findings, we assumed that amelogenin might induce the healing of injured articular cartilage. We created a large traumatic osteochondral injury (OCI) in a rat model, and studied the healing effect of rHAM+. Then we evaluated the origin of cells recruited by rHAM+ toward the defect site.

Methods

The recombinant human amelogenin protein. rHAM+ was produced according to Taylor et al[7] and stored at -80°C in 0.05 M acetic acid. Prior to use, aliquots of rHAM+ were lyophilized overnight and dissolved in 2.25% PGA carrier (KIMICA, Japan) to yield the desired concentration. At 2.25%, the PGA solution is viscous enough to be contained in the OCI without scattering over the surrounding tissues, and its fluidity enables application of an accurate dose.

Animals. The experimental protocol was approved by the ethical committee of the Hebrew University of Jerusalem (MD-21-15427-4; MD-14-14176-4). Eight-week-old female Sabra rats (n = 93), weighing 220 to 250 g, were housed in pairs under standard conditions of controlled temperature (mean 22°C (standard deviation (SD) 2)), 12-hour light/dark cycles, humidity (30% to 70%) ventilation, and ad libitum access to food and water. Rats were acclimated to a pathogen-free unit for three days, followed by handling for one week prior to operations. All rats were randomly allocated to the experimental groups using a random sequence table. Exclusion criteria were according to the ethical approval, and included clinical and/or behavioural changes. An ARRIVE checklist is included in the Supplementary Material to show our adherence to the ARRIVE guidelines.

The surgical procedure. We modified previously published models for the creation of a knee OCI in rats.[11,12] We planned and produced a machine that fixes the knee and produces a defect at a constant depth (2 mm) and diameter (1.5 mm) in the femoral trochlea with a high-speed burr (Figure 1a).

Subcutaneous tramadol (Grünenthal, Germany) was injected for pain relief prior to the operation. The surgeries were performed under isoflurane-induced anaesthesia. Through a medial parapatellar approach, the patella was everted, exposing the articular surfaces. A full-thickness OCI was created in the distal femoral trochlea. For the experimental groups, 7 µl of the following concentrations: 0.1, 0.5, 1.0, 2.5, or 5.0 µg/µl rHAM+ dissolved in 2.25% PGA were applied into the OCI. The control group was treated with 7 µl of 2.25% PGA carrier alone (Figure 1b). The surgeon was blinded to the treatment applied. The arthrotomy was sutured with interrupted 5-0 vicryl sutures, and the skin was sutured with interrupted 5-0 nylon sutures (Ethicon, USA). The rats received pain relief medication (PO dipyrone; Teva, Israel) for three days after the operation, followed by monitoring twice a week until euthanasia. The rats were euthanized with overdose of pentobarbital sodium (CTS Chemical Industries, Israel) and chest wall opening.

Study design. Sample size and timepoints for assessment were chosen based on our prior experience.[9,10] The efficacy of treatments was assessed by: 1) morphometric analysis; 2) histological analyses, 12 weeks after treatment – group sizes were as follows: 0.1 µg/µl rHAM+ (n = 7), 0.5 µg/µl rHAM+ (n = 14), 1.0 µg/µl rHAM+ (n = 8), 2.5 µg/µl rHAM+ (n = 5), 5.0 µg/µl rHAM+ (n = 6), and PGA alone

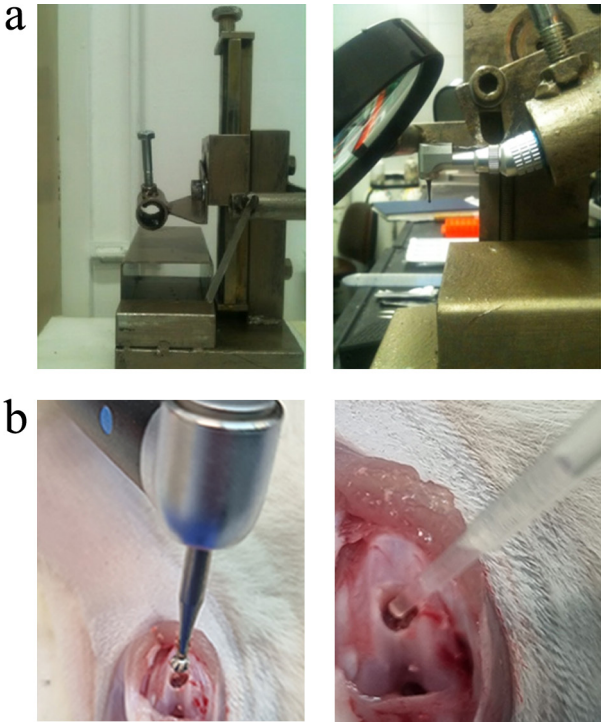

Fig. 1

a) The rat knee was fixed to a machine that creates the osteochondral injury (OCI). The depth of the OCI was determined by a screw that lowered the burr. b) Creation of OCI and application of the treatment.

(n = 14); 3) expression of the MSC marker CD105 was analyzed four days after treatment with 0.5 µg/µl rHAM+ (n = 7) or PGA (n = 8); and 4) the origin of recruited cells was also analyzed four days after treatment (six groups, n = 4 per group).

Morphometric analysis. Following euthanization, the rats' knees were photographed using Dino-Lite Digital Microscope and DinoCapture 2.0 software (Dino-Lite Digital Microscope, Taiwan). A semiquantitative macroscopic scoring system developed by Goebel et al[13] was used, based on colour, presence of blood vessels and surface of repaired tissue, OCI filling, and degeneration of adjacent cartilage. A score of 0 represents excellent cartilage repair, while 20 represents no repair and extension of the defect into adjacent cartilage.

Tissue processing and histological analyses. The distal femora were cut, fixed in 4% paraformaldehyde, and decalcified in 25% formic acid in citrate buffer until a soft consistency was achieved. The acid was then neutralized using 0.25% ammonium hydroxide, and the tissues were gradually dehydrated in ethanol, embedded in paraffin (Sakura), and cut into 5 µm-thick sections (Leica Biosystems, Germany).

Tissue anatomy of the OCI, as well as proteoglycan and types II, I, and X collagen components of the cartilage, were evaluated. Three to four slides from the middle of the OCI were used for each staining. Slides were deparaffinized, gradually hydrated, and stained using haematoxylin and eosin (H&E) (Leica Biosystems; 3801540E 3801640E), toluidine blue (MilliporeSigma, USA; 89640), or safranin O/fast green (HWI-1 (ScyTek); F7258 (MilliporeSigma); S8884 (MilliporeSigma)). For indirect immunohistochemistry, the antigen was retrieved using pronase (MilliporeSigma; 10165921001) and hyaluronidase (MilliporeSigma; H3506), unspecific binding was then blocked (Abcam ab64226) and slides were incubated with anti-type II, I, or X collagen antibodies (ab34712 (Abcam, USA), 1310-08 (SouthernBiotech, USA), or 14-977-87 (Thermo Fisher Scientific, USA), respectively). The primary antibodies were detected using ZytoChem Plus (HRP) Polymer: anti-Rabbit (Zytomed Systems, Germany; ZUC032) for type II collagen, anti-Mouse (Zytomed Systems; ZUC050) for type X collagen, or ImmPRESS HRP anti-goat Polymer (Vector Laboratories, USA; MP-7405) for type I collagen. The signal was developed using a DAB substrate kit (Cell Marque, USA; 957D). The slides were then gradually dehydrated and mounted (107961 (Merck, USA)). Repair of hyaline cartilage at the site of the OCI was semiquantitatively graded using the scale suggested by Pineda et al,[14] based on the amount of filling, reconstruction of an osteochondral junction, matrix staining, and cell morphology. A value of 0 represents complete cartilage and bone regeneration, while 14 represents no regeneration.

Evaluation of CD105-positive cells was performed using the primary antibody for CD105 (Abcam; ab231673) and the HRP-DAB micropolymer immunohistochemistry kit (Abcam; ab236469), according to the manufacturer's instructions. Three slides were stained from the middle of each OCI, and images were taken from randomly selected five fields per slide that contained the OCI and surrounding tissue, a total of 15 quantified fields per OCI.

All images were taken using a Nikon microscope (Nikon Eclipse Ti; Nikon, Japan). The analyses and quantification of all images were performed by an orthopaedic surgeon and a researcher (AH, OH) who were blinded to the treatment applied.

Evaluation of the origin of recruited cells. To evaluate the source of cells recruited toward the OCI in vivo, we used the fluorescent lipophilic cell membrane stain DiD solution (V22887; Thermo Fisher Scientific), which incorporates into cell membranes and enables in vivo tracking of cells from the injected area. Following creation of an OCI in the rats' knees and treatment with either 0.5 µg/µl rHAM+ dissolved in PGA (n = 12) or PGA alone (n = 12), rats were further randomly assigned to three groups (n = 4/group). In each group, DiD solution was injected to a different site: 2 µl DiD to a hole drilled (a) 0.5 cm or (b) 1.5 cm proximal to the OCI in the ipsilateral femur; and 3 µl DiD to the peritoneal fat pad in the left lower abdominal quadrant, which contains large quantities of MSCs.[15] The rats were euthanized four days after treatment and tissues were harvested, processed, and immunofluorescence staining was performed using antibodies against CD105 (sc-20632, Santa Cruz Biotechnology, USA) or STRO-1 (MAB1038; R&D Systems, USA), as described in Hanhan et al.[9] All slides were photographed by a researcher who was blind to the treatment applied (FS), using a Nikon microscope (Nikon Eclipse Ti).

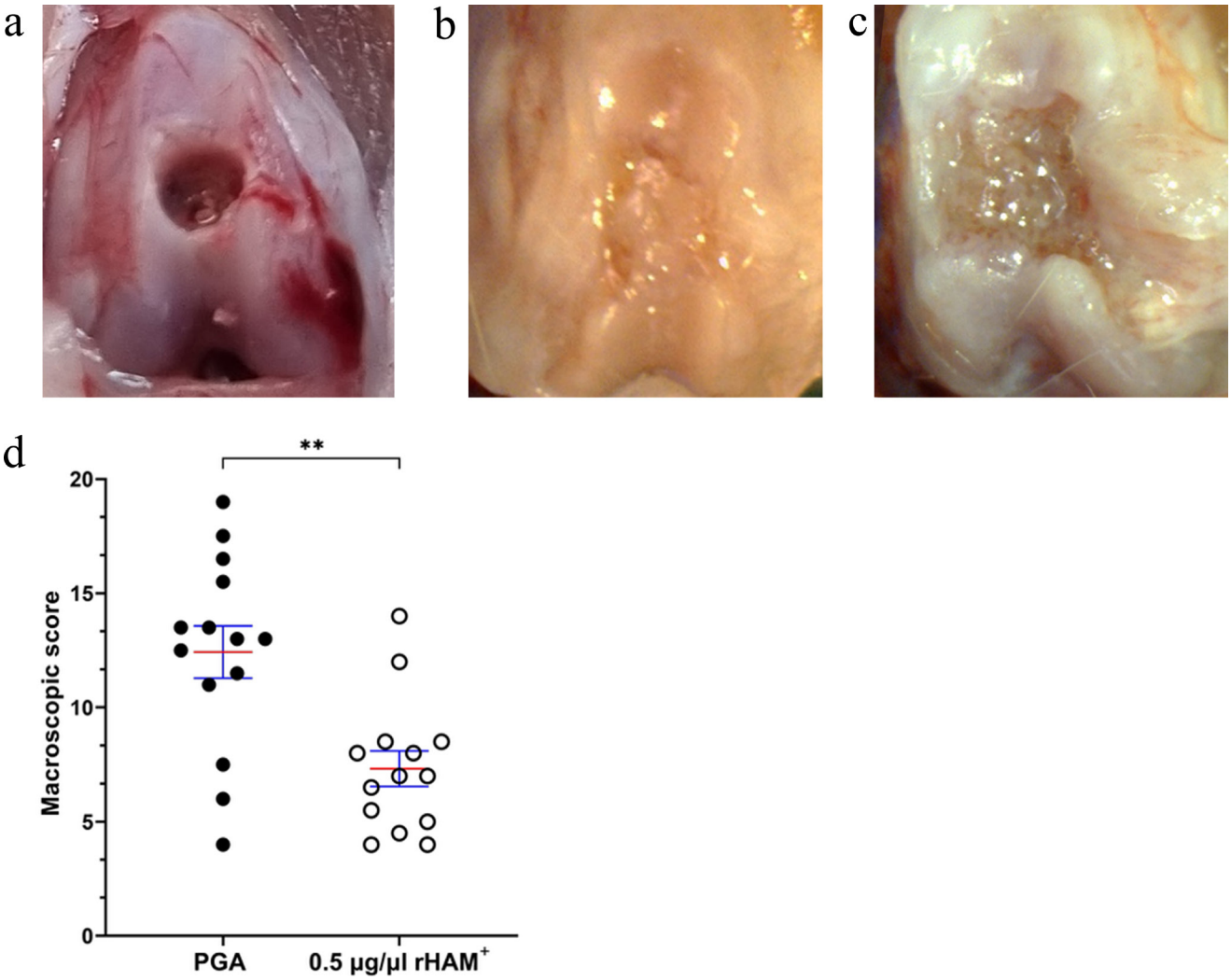

Fig. 2

Macroscopic evaluation of the osteochondral injury (OCI). Gross appearance of the OCI a) at the time of operation, and 12 weeks after operation and application of b) 0.5 µg/µl recombinant human amelogenin protein (rHAM+) and c) propylene glycol alginate (PGA). d) Scoring of the OCI 12 weeks after treatment with 0.5 µg/µl rHAM+ (n = 14) or PGA (n = 14), performed according to Goebel et al's[13] classification. Data are presented as mean (standard error of the mean). **p < 0.01, Mann-Whitney U test. The images represent tissues scored around mean values for each group.

Statistical analysis. Statistical analyses were performed using the GraphPad Prism 9 software (GraphPad Software, USA). The data were compared using Kruskal-Wallis one-way analysis of variance or Mann-Whitney U test, as depicted. The data are presented as mean value and standard error of the mean (SEM). A p-value < 0.05 was considered to be statistically significant.

Results

Articular cartilage repair. Macroscopic evaluation: macroscopic grading of the OCI, performed 12 weeks after treatment, revealed that in the rHAM+-treated group, the defect was predominantly filled with white heterogeneous surface tissue, which was integrated, partially in-line, with the surrounding cartilage. Conversely, in the PGA-treated group, the size of the defect increased, minimal repair tissue was detected, and post-traumatic degenerative changes, such as large fissures and fibrillation mixed with ulceration resembling rapid post-traumatic osteoarthritis (OA), were observed in the defect site and surrounding cartilage (Figures 2a to 2c). Semiquantitative macroscopic scoring, according to Goebel et al,[13] showed a significantly better score, representing better cartilage repair after treatment with 0.5 µg/µl rHAM+, compared to treatment with PGA carrier alone (mean 7.32 (SE 0.78) vs mean 12.43 (SE 1.14), respectively; p < 0.01, Mann-Whitney U test) (Figure 2d).

Histological evaluation: 12 weeks after treatment, the OCIs were evaluated by H&E staining for general histology, toluidine blue and safranin O staining for proteoglycan content, and immunohistochemistry for type II, I, and X collagens. Significant healing of the subchondral bone was observed in the experimental 0.5 µg/µl rHAM+-treated group. The hyaline cartilage gradually healed from the

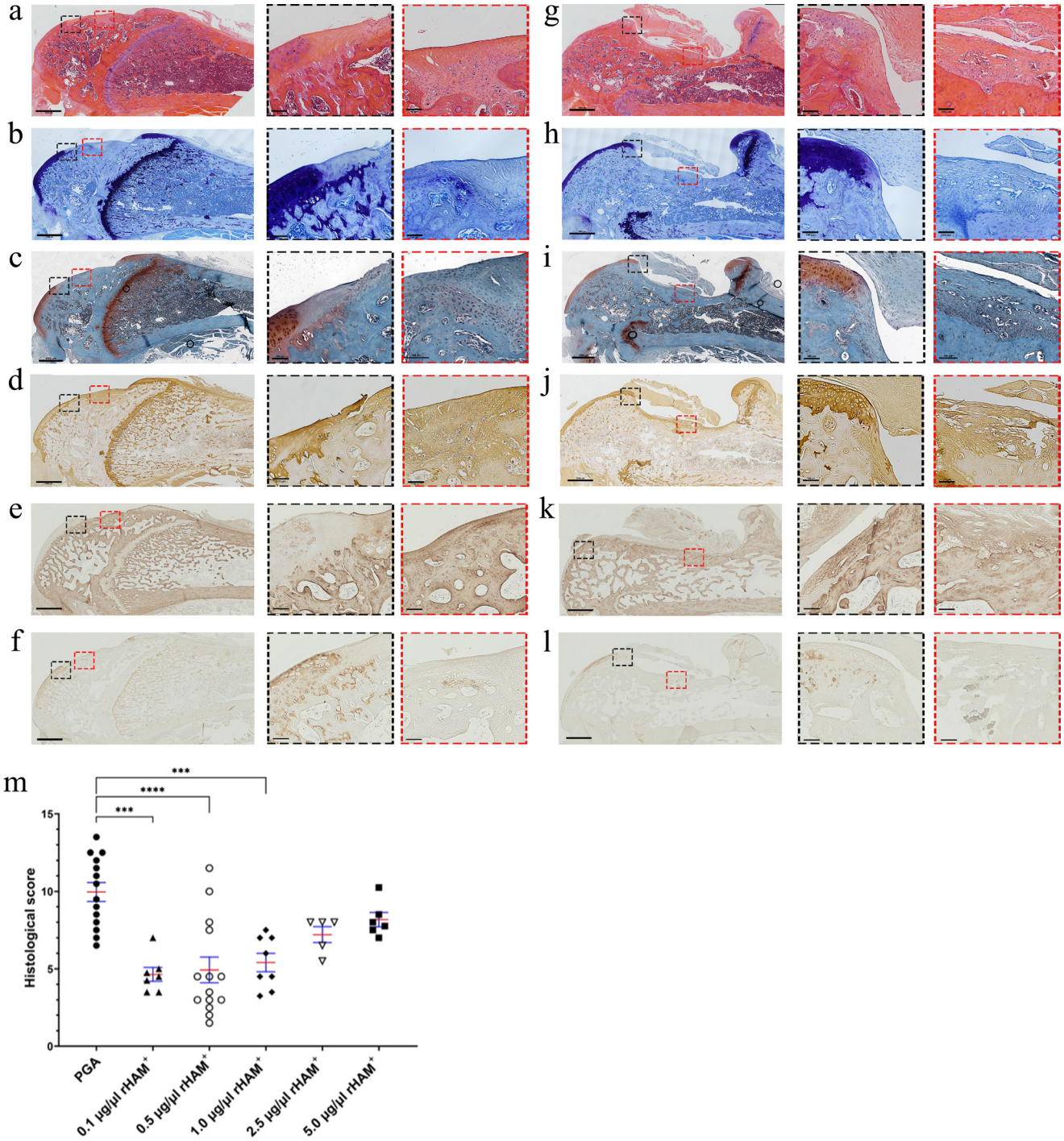

Fig. 3

Histological analyses of the osteochondral injury (OCI) 12 weeks after treatment, with recombinant human amelogenin protein (rHAM⁺) dissolved in propylene glycol alginate (PGA) or only PGA carrier. a) to f) OCI treated with 0.5 µg/µl rHAM⁺; g) to l) OCI treated with PGA. a) and g) haematoxylin and eosin (H&E) staining; b) and h) Toluidine blue staining; c) and i) safranin O/fast green staining. Immunohistochemistry staining was used for: d) and j) type II collagen; e) and k) type I collagen; and f) and i) type X collagen. Scale bar: 100 µm. Enlarged pictures (×10) were taken from the regions marked with red and black frames. Black frames represent the edge of the defect, while red frames represent the centre of the OCI. m) Histological grading of the OCI after treatment with 0.1 µg/µl rHAM⁺ (n = 7), 0.5 µg/µl rHAM⁺ (n = 14), 1.0 µg/µl rHAM⁺ (n = 8), 2.5 µg/µl rHAM⁺ (n = 5), 5.0 µg/µl rHAM⁺ (n = 6), and PGA alone (n = 14). Grading was performed according to Pineda et al's scoring system.[14] Data are presented as mean (standard error of the mean). ***p < 0.001, ****p < 0.0001; Kruskal-Wallis one-way analysis of variance. The images represent tissues scored around mean values and were taken from the same rats presented in Figure 2.

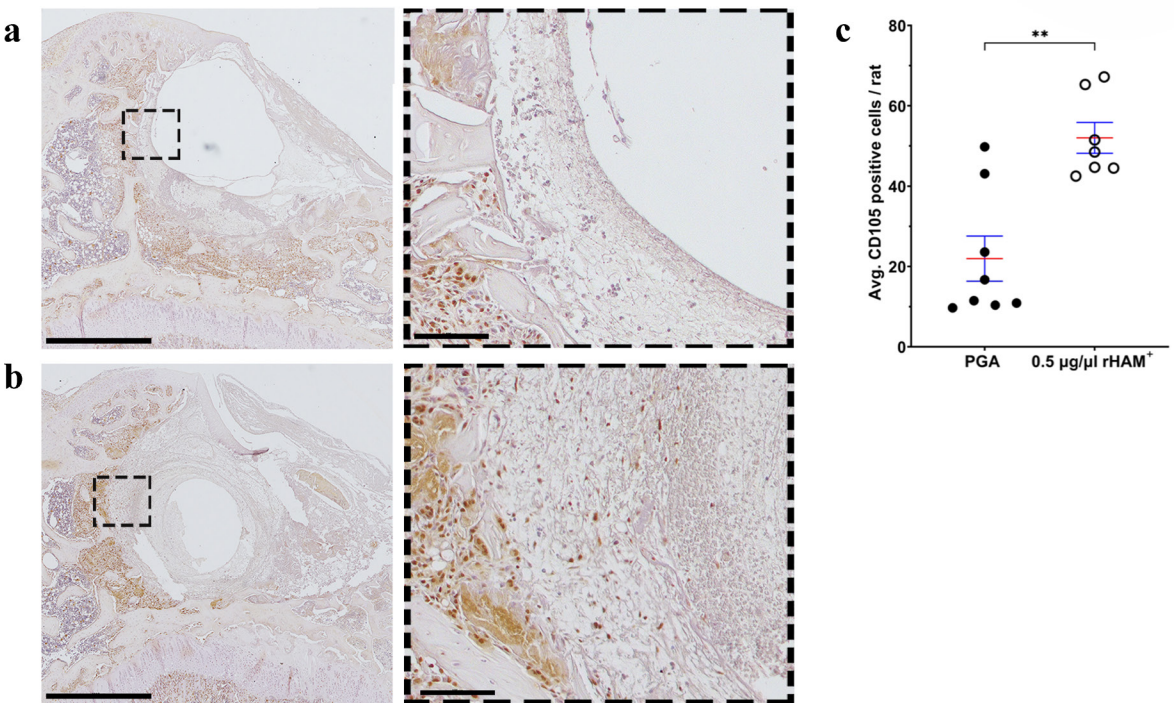

Fig. 4

Histological analysis of the granulation tissue at the osteochondral injury (OCI) four days after treatment. Immunohistochemistry for CD105 expression after treatment with a) propylene glycol alginate (PGA) alone (n = 8) and b) 0.5 µg/µl recombinant human amelogenin protein (rHAM+) (n = 7). Scale bar: 1,000 µm. Enlarged pictures (×20) were taken from the regions marked with black frames, scale bar: 100 µm. Brown staining: CD105 positive cells; purple staining (haematoxylin and eosin (H&E)): CD105 negative cells. c) Average number of cells in the granulation tissue and surrounding of the OCI. Data presented as mean (standard error of the mean). **p < 0.01, Mann-Whitney U test.

deeper layers of the defect toward the surface and from the edges toward the centre of the defect. The deeper layers and the edges were better arranged than the superficial layers, depicting chondrocytes embedded in their lacunae and osteochondral junction growth (Figure 3a). Considerably larger amounts of proteoglycans and type II collagen in the extracellular matrix were evident in the deep layers of the newly formed cartilage and at the edges of the defect (Figures 3b to 3d, Supplementary Figure a). Reduced expression of type I collagen was observed at the cartilaginous boundary (Figures 3e and 3k). At the centre of the defect, however, higher expression of the type I collagen was detected, demonstrating the ongoing process of bone formation and incomplete healing of the articular cartilage (Figure 3e). Yet, type X collagen appeared at the border between the subchondral bone and the forming cartilaginous tissue after treatment with rHAM+, further indicating maturation of the subchondral bone and the development of a calcified zone and tide mark (Figure 3f). By contrast, in the control PGA-treated group, larger defects were observed (Figure 3g). In the tissue surrounding the defect, cartilage fractures and areas of minimal staining for proteoglycans and type II collagen, as well as high staining for type I collagen, were depicted (Figures 3h to 3k). Additionally, no type X collagen was detected in the defect or at the interface between the subchondral bone and the superficial fibrotic tissue (Figure 3l). These findings suggest the production of fibrous tissue formation and post-traumatic osteoarthritic alterations at the OCI and surrounding area.

Semiquantitative analysis of the histological changes was performed according to Pineda et al's[14] classification (Figure 3m). The experimental groups treated with 0.1 to 1.0 µg/µl rHAM+ obtained significantly better scores ($p < 0.001$; Kruskal-Wallis one-way ANOVA) compared to the control group treated with PGA carrier alone (0.1 µg/µl rHAM+, mean 4.64 (SEM 0.45); 0.5 µg/µl rHAM+, mean 4.93 (SEM 0.83); 1.0 µg/µl rHAM+, mean 5.41 (SE 0.60)) versus PGA (mean 9.96 (SEM 0.61)), which represents better healing of the OCI. The higher concentrations of 2.5 µg/µl and 5 µg/µl rHAM+ obtained better scores compared to the control group (2.5 µg/µl rHAM+, mean 7.2 (SE 0.50); 5 µg/µl rHAM+, mean 8.17 (SE 0.50)), however the improvement was not significant. Since the best healing was observed after treatment with 0.5 µg/µl rHAM+, we decided to continue using this concentration in subsequent experiments.

Paracrine recruitment of cells expressing MSC markers. Recent studies attempted to regenerate OCIs with various combinations of chemoattractants and scaffolds, aiming to recruit endogenous cells.[3] CD105 (endoglin)

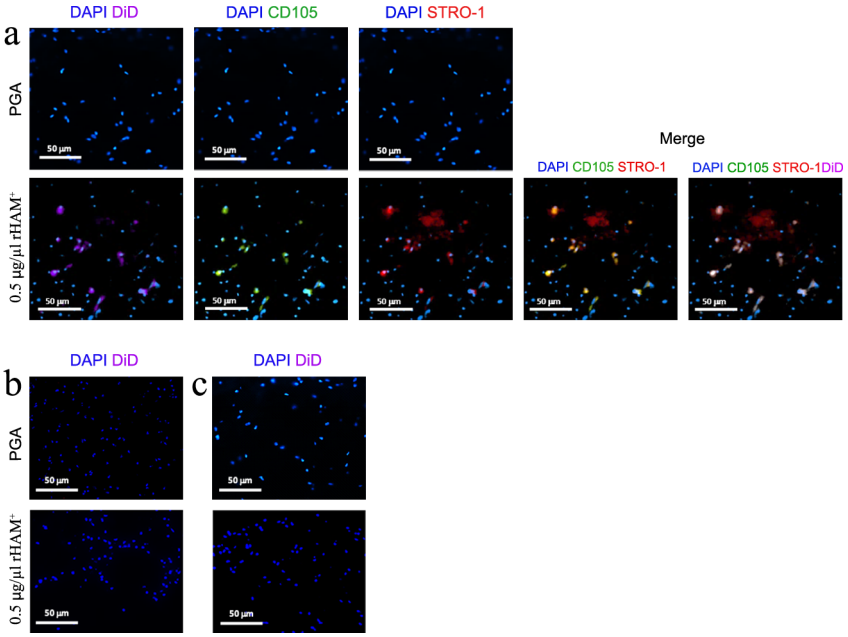

Fig. 5

In vivo cell tracking four days after creation of an osteochondral injury (OCI) at the rat's knee, and treatment with 0.5 µg/µl recombinant human amelogenin protein (rHAM+) or with propylene glycol alginate (PGA) carrier. Following the creation of an OCI at the rat's knee, DiD was injected into a hole drilled a) 0.5 cm proximal or b) 1.5 cm proximal to the OCI in the ipsilateral femur, or c) to the peritoneal fat pad (total six groups, n = 4 per group). Immunofluorescence staining was performed as depicted in the heading of each image. Cell nuclei were stained with 4',6-diamidino-2-phenylindole (DAPI). Staining for DiD, CD105, and STRO-1 was observed only in the picture taken from the OCI when DiD was injected 0.5 cm proximal to the defect. Scale bar: 50 µm.

is expressed on the membrane of joint- and peritoneal-resident stem cells.[3,16] Hence, we evaluated the expression of CD105 in the OCI four days after treatment. Significantly more CD105-positive cells were seen in the OCI and surrounding tissue after treatment with 0.5 µg/µl rHAM+ than in the control treated with PGA (mean 21.96 (SEM 5.62) vs mean 52.03 (SEM 3.84), respectively; $p < 0.01$, Mann-Whitney U test) (Figure 4). This suggests that rHAM+ specifically recruits CD105-positive cells to the injured site, as seen in our previous in vivo models.[8-10]

We next evaluated the origin of the recruited cells. Following the creation of an OCI in the rats' knees and treatment with 0.5 µg/µl rHAM+ or PGA alone, the fluorescent DiD solution, which incorporates into cell membranes and enables tracking of cells from the injected area, was injected into an additional hole drilled 0.5 cm or 1.5 cm proximal to the OCI in the ipsilateral femur (paracrine recruitment) or to the abdominal peritoneal fat pad (endocrine recruitment). Immunofluorescent staining of thin sections of the knees' OCIs four days after treatment was performed for CD105, STRO-1 (expressed on stem cells). DiD (recruited cell marker) was detected only in the granulation tissue of the rHAM+-treated group, to which DiD was administered 0.5 cm proximal to the OCI (Figure 5a). However, no DiD was observed following rHAM+ treatment, when DiD was injected 1.5 cm proximal to the OCI, or at the peritoneal fat pad (Figures 5b and 5c). In addition, no cells expressing DiD were observed in the three control groups treated with PGA (Figures 5a to 5c). This indicates that rHAM+ induces paracrine recruitment of cells expressing MSC markers only from the adjacent bone marrow.

Discussion

Here, we describe a reproducible in vivo model of rat OCI. This model enabled us to evaluate the effect of various concentrations of rHAM+ on the healing of the OCI 12 weeks after the operation.

Previous studies demonstrated a limited or no effect of full-length amelogenin on bone regeneration.[17] Several amelogenin-derived peptides promote bone formation in vitro; however, studies on their effect on in vivo bone formation are inconclusive.[18] Here we showed that treatment with 0.5 µg/µl rHAM+, the concentration that yielded the best regenerative effect in this and our previous studies,[9,10] brought about healing of the subchondral bone, which serves as the matrix nourishing and supporting hyaline cartilage. Indeed, superficial to the subchondral bone, a tissue resembling partially differentiated hyaline cartilage was observed. The newly formed cartilage exhibited gradual healing, noticeable in both the peripheral zone and deeper layers of the defect, resembling the natural process. Higher expression of proteoglycans and type II collagen, the hallmark of hyaline cartilage, was predominantly detected at the defect edges, while type I collagen expression was primarily observed at the centre, indicating the ongoing process of bone healing and the differentiation from fibrocartilage into hyaline cartilage. Additionally, the expression pattern of type X collagen at the base of the defect

in the rHAM+-treated OCI indicated maturation of the subchondral bone and the establishment of a tide mark demarcating the boundary between the bone and developing cartilage. In contrast, the PGA-treated OCIs yielded changes observed in rapid post-traumatic OA. These changes were characterized by substantially damaged tissues, a marked reduction in proteoglycan secretion, and no osteochondral junction growth. Notably, elevated expression of type I collagen, known to be upregulated during OA, was observed in the proximity of the defect.

The expression of CD105 is one of the essential criteria for the definition of MSCs.[19] It is additionally expressed in other cells, such as pericyte endothelial cells.[20] Given the well-established correlation between CD105-positive cells and high chondrogenic potential,[21] we evaluated the expression of CD105-positive cells at the OCIs four days after treatment with rHAM+. The results show that rHAM+ induced a significant increase in the number of CD105-expressing cells within the granulation tissue of the OCI four days after treatment. Although the exact identity of the CD105-positive cells needs to be further evaluated, it is reasonable to speculate that this population includes MSCs or cells differentiating from MSCs (including chondroblasts). MSCs exhibit pleiotropic effects, including migration and homing, anti-inflammatory and immunomodulatory properties, and differentiate to promote tissue repair.[22] In vitro studies demonstrated that amelogenin can induce cell migration.[23] Indeed, we identified paracrine migration of cells expressing the MSC markers CD105 and STRO-1 into the OCI only from the adjacent ipsilateral proximal femur. No endocrine systemic effect was detected. Following cartilage injury, joint-resident MSCs (subchondral bone, synovium, synovial fluid, and adipose tissue) are naturally recruited into cartilage lesions to restore morphology and function.[3,24] However, this natural recruitment mechanism is often insufficient for repair.[3,24] Notably, microfracture surgery, which involves the creation of perforations in the subchondral bone plate to facilitate the migration of bone marrow-derived MSCs into small lesions,[25] does not bring about cartilage regeneration but the creation of fibrocartilage.[25,26] Hence, cell recruitment by itself is insufficient for regeneration. Chemokines are secreted during injury and enhance the migration of endogenous stem cells to the site of injury. However, during a natural healing response, the amount and extent of chemoattractants are limited, insufficient for regeneration.[27] We propose that rHAM+, as a chemoattractant, enhances the natural mechanism of endogenous stem cell recruitment following cartilage injury. Furthermore, we have previously demonstrated that rHAM+ facilitated cell proliferation in vivo,[9] in addition to the in vitro induction of proliferation of bone marrow-derived MSCs and other types of cells by amelogenin.[28,29] Thereby, the proliferative abilities of amelogenin, together with the migratory effect presented here, augment tissue healing. Additional studies are required to reveal the molecular mechanisms underlying the healing process of injured mesenchymal tissues, mediated by amelogenin.

In summary, our study showed that rHAM+ induced healing of injured articular cartilage and underlying subchondral bone, and prevented destructive post-traumatic osteoarthritic changes by promoting paracrine recruitment of endogenous cells expressing the mesenchymal stem cell marker CD105. Thus, amelogenin can be further evaluated in a large animal model for the treatment of cartilage injuries.

Supplementary material

Figure showing histological analyses of the osteochondral injury 12 weeks after treatment with recombinant human amelogenin protein dissolved in propylene glycol alginate. An ARRIVE checklist is also included to show that the ARRIVE guidelines were adhered to in this study.

References

1. **Armiento AR**, **Alini M**, **Stoddart MJ**. Articular fibrocartilage - Why does hyaline cartilage fail to repair? *Adv Drug Deliv Rev*. 2019;146:289–305.
2. **Everhart JS**, **Abouljoud MM**, **Flanigan DC**. Lateral cartilage defects and medial subchondral surface ratio are associated with knee-related disability. *J Orthop Res*. 2019;37(2):378–385.
3. **Yang Z**, **Li H**, **Yuan Z**, **et al**. Endogenous cell recruitment strategy for articular cartilage regeneration. *Acta Biomater*. 2020;114:31–52.
4. **Le H**, **Xu W**, **Zhuang X**, **Chang F**, **Wang Y**, **Ding J**. Mesenchymal stem cells for cartilage regeneration. *J Tissue Eng*. 2020;11:1–22.
5. **Tamaddon M**, **Blunn G**, **Xu W**, **et al**. Sheep condyle model evaluation of bone marrow cell concentrate combined with a scaffold for repair of large osteochondral defects. *Bone Joint Res*. 2021;10(10):677–689.
6. **Haze A**, **Taylor AL**, **Blumenfeld A**, **et al**. Amelogenin expression in long bone and cartilage cells and in bone marrow progenitor cells. *Anat Rec (Hoboken)*. 2007;290(5):455–460.
7. **Taylor AL**, **Haze-Filderman A**, **Blumenfeld A**, **et al**. High yield of biologically active recombinant human amelogenin using the baculovirus expression system. *Protein Expr Purif*. 2006;45(1):43–53.
8. **Haze A**, **Taylor AL**, **Haegewald S**, **et al**. Regeneration of bone and periodontal ligament induced by recombinant amelogenin after periodontitis. *J Cell Mol Med*. 2009;13(6):1110–1124.
9. **Hanhan S**, **Ejzenberg A**, **Goren K**, **et al**. Skeletal ligament healing using the recombinant human amelogenin protein. *J Cell Mol Med*. 2016;20(5):815–824.
10. **Hanhan S**, **Goren K**, **Rivkin A**, **et al**. Regeneration of grade 3 ankle sprain, using the recombinant human amelogenin protein (rHAM+) in a rat model. *J Orthop Res*. 2021;39(7):1540–1547.
11. **Hori J**, **Deie M**, **Kobayashi T**, **Yasunaga Y**, **Kawamata S**, **Ochi M**. Articular cartilage repair using an intra-articular magnet and synovium-derived cells. *J Orthop Res*. 2011;29(4):531–538.
12. **Xue D**, **Zheng Q**, **Zong C**, **et al**. Osteochondral repair using porous poly(lactide-co-glycolide)/nano-hydroxyapatite hybrid scaffolds with undifferentiated mesenchymal stem cells in a rat model. *J Biomed Mater Res A*. 2010;94(1):259–270.
13. **Goebel L**, **Orth P**, **Cucchiarini M**, **Pape D**, **Madry H**. Macroscopic cartilage repair scoring of defect fill, integration and total points correlate with corresponding items in histological scoring systems - a study in adult sheep. *Osteoarthritis Cartilage*. 2017;25(4):581–588.
14. **Pineda S**, **Pollack A**, **Stevenson S**, **Goldberg V**, **Caplan A**. A semiquantitative scale for histologic grading of articular cartilage repair. *Acta Anat (Basel)*. 1992;143(4):335–340.
15. **Posada-González M**, **Villagrasa A**, **García-Arranz M**, **et al**. Comparative analysis between mesenchymal stem cells from subcutaneous adipose tissue and omentum in three types of patients: Cancer, morbid obese and healthy control. *Surg Innov*. 2022;29(1):9–21.
16. **Cohen CA**, **Shea AA**, **Heffron CL**, **Schmelz EM**, **Roberts PC**. Intra-abdominal fat depots represent distinct immunomodulatory microenvironments: a murine model. *PLoS One*. 2013;8(6):e66477.

17. **Donos N**, **Dereka X**, **Calciolari E**. The use of bioactive factors to enhance bone regeneration: A narrative review. *J Clin Periodontol*. 2019;46 Suppl 21:124–161.
18. **Fiorino A**, **Marturano A**, **Placella G**, **et al**. Amelogenin-derived peptides in bone regeneration: A systematic review. *Int J Mol Sci*. 2021;22(17):17.
19. **Dominici M**, **Le Blanc K**, **Mueller I**, **et al**. Minimal criteria for defining multipotent mesenchymal stromal cells. The International Society for Cellular Therapy position statement. *Cytotherapy*. 2006;8(4):315–317.
20. **Zhang ZS**, **Zhou HN**, **He SS**, **Xue MY**, **Li T**, **Liu LM**. Research advances in pericyte function and their roles in diseases. *Chin J Traumatol*. 2020;23(2):89–95.
21. **Qi J**, **Chen A**, **You H**, **Li K**, **Zhang D**, **Guo F**. Proliferation and chondrogenic differentiation of CD105-positive enriched rat synovium-derived mesenchymal stem cells in three-dimensional porous scaffolds. *Biomed Mater*. 2011;6(1):015006.
22. **Merimi M**, **El-Majzoub R**, **Lagneaux L**, **et al**. The therapeutic potential of mesenchymal stromal cells for regenerative medicine: Current knowledge and future understandings. *Front Cell Dev Biol*. 2021;9:661532.
23. **Toyoda K**, **Fukuda T**, **Sanui T**, **et al**. Grp78 is critical for amelogenin-induced cell migration in a multipotent clonal human periodontal ligament cell line. *J Cell Physiol*. 2016;231(2):414–427.
24. **McGonagle D**, **Baboolal TG**, **Jones E**. Native joint-resident mesenchymal stem cells for cartilage repair in osteoarthritis. *Nat Rev Rheumatol*. 2017;13(12):719–730.
25. **Medina J**, **Garcia-Mansilla I**, **Fabricant PD**, **Kremen TJ**, **Sherman SL**, **Jones K**. Microfracture for the treatment of symptomatic cartilage lesions of the knee: A survey of International Cartilage Regeneration & Joint Preservation Society. *Cartilage*. 2021;13(1_suppl):1148S–1155S.
26. **DiBartola AC**, **Everhart JS**, **Magnussen RA**, **et al**. Correlation between histological outcome and surgical cartilage repair technique in the knee: A meta-analysis. *Knee*. 2016;23(3):344–349.
27. **Andreas K**, **Sittinger M**, **Ringe J**. Toward in situ tissue engineering: chemokine-guided stem cell recruitment. *Trends Biotechnol*. 2014;32(9):483–492.
28. **Huang Y-C**, **Tanimoto K**, **Tanne Y**, **et al**. Effects of human full-length amelogenin on the proliferation of human mesenchymal stem cells derived from bone marrow. *Cell Tissue Res*. 2010;342(2):205–212.
29. **Kunimatsu R**, **Tanimoto K**, **Tanne Y**, **et al**. Amelogenin enhances the proliferation of cementoblast lineage cells. *J Periodontol*. 2011;82(11):1632–1638.

Author information:
- O. Helwa-Shalom, MSc, PhD Student
- S. I. Markowitz, MSc, PhD Student
  The inter-faculty Biotechnology Program, The Hebrew University of Jerusalem, Jerusalem, Israel.
- F. Saba, DMD, PhD, Researcher
- S. Hanhan, DMD, PhD, Researcher
- K. Goren, PhD, Researcher
- D. Shilo, DMD, PhD, Researcher
- D. Deutsch, PhD, Professor
  Faculty of Dental Medicine, The Hebrew University of Jerusalem, Jerusalem, Israel.
- E. Spitzer, MD, Orthopedic Surgeon
- N. Khaimov, MD, Orthopedic Surgeon
- Y. N. Gellman, MD, Orthopedic Surgeon
  Orthopedic Surgery Department, Hadassah University Medical Center, Jerusalem, Israel.
- A. Blumenfeld, PhD, Researcher, Faculty of Dental Medicine, The Hebrew University of Jerusalem, Jerusalem, Israel; The Wohl Institute for Translational Medicine, Hadassah University Medical Center, Jerusalem, Israel.
- H. Nevo, PhD, Researcher, Orthopedic Surgery Department, Hadassah University Medical Center, Jerusalem, Israel; The Wohl Institute for Translational Medicine, Hadassah University Medical Center, Jerusalem, Israel.
- A. Haze, MD, PhD, Orthopedic Surgeon, Principal Investigator, Orthopedic Surgery Department, Hadassah University Medical Center, Jerusalem, Israel; The Wohl Institute for Translational Medicine, Hadassah University Medical Center, Jerusalem, Israel; Faculty of Medicine, The Hebrew University of Jerusalem, Jerusalem, Israel.

Author contributions:
- O. Helwa-Shalom: Investigation, Formal analysis, Methodology, Visualization, Writing – original draft.
- F. Saba: Conceptualization, Methodology, Investigation, Formal analysis, Writing – original draft.
- E. Spitzer: Methodology, Investigation.
- S. Hanhan: Methodology, Investigation.
- K. Goren: Investigation, Resources, Formal analysis.
- S. I. Markowitz: Investigation, Visualization.
- D. Shilo: Investigation, Formal analysis.
- N. Khaimov: Conceptualization, Methodology.
- Y. N. Gellman: Methodology, Writing – review & editing.
- D. Deutsch: Conceptualization, Supervision, Validation, Writing – original draft.
- A. Blumenfeld: Funding acquisition, Conceptualization, Project administration, Methodology, Supervision, Writing – original draft, Writing – review & editing.
- H. Nevo: Methodology, Validation, Visualization, Investigation, Supervision, Writing – original draft, Writing – review & editing, Project administration, Resources.
- A. Haze: Conceptualization, Funding acquisition, Supervision, Methology, Formal analysis, Validation, Writing – original draft, Writing – review & editing.

- O. Helwa-Shalom and F. Saba contributed equally to this work.

Funding statement:
- The authors disclose receipt of the following financial or material support for the research, authorship, and/or publication of this article: funding from the AO foundation, grant number S-13-96H; the Israeli Innovation Authority - Magneton grant, grant number 73707; and a donation to Hadassah University Medical Center, internal number 6069195. The funding source had no role in: the study design or collection, analysis, and interpretation of data; the writing of the manuscript; or in the decision to submit the manuscript for publication.

ICMJE COI statement:
- The authors declare that they have no competing interests.

Data sharing:
- The data that support the findings for this study are available to other researchers from the corresponding author upon reasonable request.

Ethical review statement:
- All procedures were approved by the Institutional Animal Care and Use Committee at the Hebrew University of Jerusalem, Israel.

Open access funding:
- The authors report that they received open access funding for their manuscript from a donation made to Hadassah University Medical Center, internal number 6069195.